Precision Agric (2014) 15:523–531
DOI 10.1007/s11119-014-9350-0

Combination active optical and passive thermal infrared sensor for low-level airborne crop sensing

D. W. Lamb · D. A. Schneider · J. N. Stanley

Published online: 14 February 2014

Abstract An integrated active optical, and passive thermal infrared sensing system was deployed on a low-level aircraft (50 m AGL) to record and map the simple ratio (SR) index and canopy temperature of a 230 ha cotton field. The SR map was found to closely resemble that created by a RapidEye satellite image, and the canopy temperature map yielded values consistent with on-ground measurements. The fact that both the SR and temperature measurements were spatially coincident facilitated the rapid and convenient generation of a direct correlation plot between the two parameters. The scatterplot exhibited the typical reflectance index-temperature profile generated by previous workers using complex analytical techniques and satellite imagery. This sensor offers a convenient and viable alternative to other forms of optical and thermal remote sensing for those interested in plant and soil moisture investigations using the 'reflectance index-temperature' space concept.

Keywords Active optical sensing · Thermal infrared · Normalised difference vegetation index · Simple ratio index · Plant and soil moisture status

Introduction

Active, optical plant canopy sensors are devices that, by virtue of integrated light sources, irradiate a target and record the reflected portion returning to similarly integrated detectors. Generally the sources are modulated, allowing synchronous detection electronics that renders the recorded information independent of changes in ambient light conditions. Such sensors can even be operated at night. These sensors, with source wavelengths ranging from blue through to near infrared wavelengths ($\approx$450–850 nm) are finding increasing use

D. W. Lamb (✉) · D. A. Schneider · J. N. Stanley
Cooperative Research Centre for Spatial Information and Precision Agriculture Research Group, University of New England, Armidale, NSW 2351, Australia
e-mail: dlamb@une.edu.au

in agriculture, with applications ranging from quantifying the nutritional requirements of crops (Inman et al. 2005; Solari et al. 2008; Holland and Schepers 2010, 2013; Barker and Sawyer 2012), as a basis for applying agrochemicals in real-time (Holland and Schepers 2013; Falzon et al. 2012) and as an objective biomass assessment tool in pastures (Künnemeyer et al. 2001; Trotter et al. 2010). The physical and radiometric principles governing the use of proximal, active optical sensors has been presented elsewhere (Holland et al. 2012).

Recently, researchers reported on the testing of these sensors in low level aircraft at altitudes ranging from 4 m (Lamb et al. 2009) up to 50 m (Lamb et al. 2011) above crop canopies. The advantages of airborne deployment of these sensors includes time saving, scale of coverage, integration with existing airborne operations such as top-dressing and avoiding the damage to established crops resulting from on-ground vehicle surveys.

The use of thermal infrared (TIR) wavelengths to infer plant canopy or leaf temperature is an important source of information to infer plant transpiration rates, and through this, biophysical parameters such as stomatal conductance. Measured either using TIR thermometers, and more recently TIR imaging, they can be used to delineate moisture stress in plants with applications for irrigation scheduling (Jackson et al. 1981; Blum et al. 1982; Pinter et al. 1990; Jones 2004; Jones et al. 2009; Wang et al. 2010). Previous work has examined the combination of surface temperature (T_s) and reflectance-based indices like the normalized difference vegetation index (NDVI) as an indicator of vegetation stress (Moran et al. 1994), and more recent work involving the MODIS satellite on the so-called NDVI-T_s space has demonstrated the ability to infer soil moisture status (Patel et al. 2009).

This paper reports on a recent trial to evaluate an integrated system for low-level airborne deployment comprising of passive TIR and active optical sensor components, with a view to offering an alternative sensor platform/system to satellites and on-ground radiometry for researchers and end-users interested in plant and soil moisture status monitoring.

Materials and methods

The sensor used for the trial was an ACS-225LR-IRT ('Raptor MkII', Holland Scientific, Lincoln, NE, USA) constructed specifically for this purpose. The sensor head comprises two separate components; an active optical component and a passive TIR detector.

The active optical component comprises 12 high-radiance LEDS, utilising the modulated polychromatic configuration of Holland et al. (2004), emitting in wavelengths of 660 nm (Red) and 850 nm (NIR). Owing to the single cylindrical lens in the front of the diode array (labelled 'A' in Fig. 1), the Raptor sensor also provides a uniform irradiance footprint with a divergence angle of approximately 14° × 8° as bounded by the half-power extremes of the irradiance footprint. The detector (labelled 'B' in Fig. 1) field-of-view (FOV) is defined by the irradiance footprint (Holland et al. 2012) and this component of the sensor is essentially that described earlier by Lamb et al. (2011). The passive TIR sensor component is a miniature thermopile detector (labelled 'C' in Fig. 1), with a spectral response range between 6–4 μm and a 5 mm diameter input aperture. The TIR sensor FOV is circular with a cone angle of approximately 12°.

As with the previous trials (Lamb et al. 2009, 2011), the Raptor MkII was mounted underneath a Fletcher FU24954 crop-dusting aircraft, positioned with a nadir view and orientated with the long axis of the LED array at right angles to the direction of flight (Fig. 1). The sensor head was connected to a GeoSCOUT GLS 400 datalogger (Holland

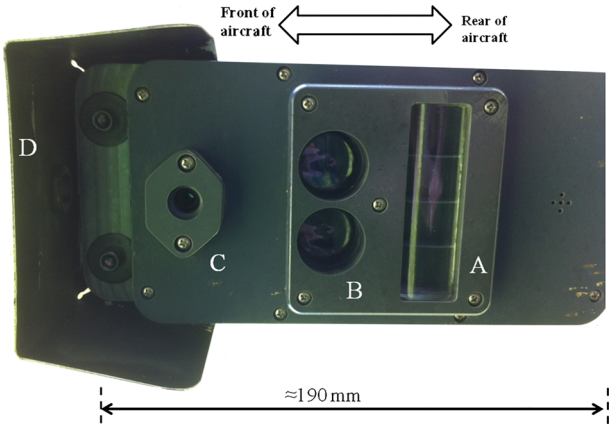

Fig. 1 The ACS-225LR-IRT (Raptor MKII) sensor head mounted on the aircraft. Key optical features include the polychromatic source (*A*), the Red and NIR detectors (*B*), the passive thermopile detector (*C*) and the shroud (*D*)

Scientific, Lincoln NE USA) and positional information was provided into the same datalogger by a 5 Hz global positioning system (Garmin GPS18 × 5 Hz, Olathe, KA, USA). As discussed by Lamb et al. (2009), this GPS-datalogger combination, given the GeoSCOUT linearly interpolates positions between the 5 Hz sample locations, provides an effective 17 Hz position calculation rate. At this sample rate, and a forward speed of 108 knots (54 m s^{-1}) used in this present work, this equates to 3.1 m translation distance between samples.

Instantaneous Red and NIR values from the active optical sensor were converted to the simple ratio (SR) vegetation index according to $\mathrm{SR} = \frac{\mathrm{NIR}}{\mathrm{Red}}$ (Jordan 1969). This index was selected owing to the fact that it, and similar variants such as the Chlorphyll Red Index (CI SR−1), does not saturate at high leaf area index (LAI) in crops (Holland and Schepers 2011). The passive thermal sensor voltages were converted to temperature (°C) based on a canopy emissivity of 0.95 (Jones et al. 2003 and references therein).

Aerial surveys were conducted on 5th February 2013 over a 230 ha field of cotton (*Gossypium hirsutum*) at growth stage '6 nodes above white flower' corresponding to a fully-closed canopy of approximately 1.3 m height above the soil. The survey site was located on the property "Keytah" (Sundown Pastoral Company P/L, paddocks L2 and L4) located 30 km west of Moree, in the northwest region of New South Wales, Australia (Latitude 29°31′9.04″S, Longitude: 149°35′52.22″E).

Flights were conducted over the field along pre-programmed, 20 m transects (approximately north–south) at an altitude of 50 m above the crop canopy and at a ground speed of approximately 54 m s^{-1} (108 knots indicated airspeed). The on-ground sensing footprint of the active optical sensor at this altitude was a rectangle approximately 7 m (along) × 12 m (across), and for the passive thermal sensor was circular of 10 m diameter. Commencing at 10.45 am (AEST) time, the survey took approximately 75 min to complete. Given the lateral offset of the sensors on the aircraft (∼1 cm) and the physical dimensions of the sensor footprints on the ground (∼10 m), the sensor footprints were coincident on the ground.

Both the visible and thermal transect data were rendered into full-field maps by first block-kriging using a 20 m block size (to encapsulate both the visible and thermal sensor

footprint of the Raptor) and a local semi-variogram model, as provided in the computer program Vesper (Whelan et al. 2001). Throughout the survey period, on-ground, spot measurements of temperature were completed at 30 min intervals, for both the cotton canopy and bare soil, using a handheld TIR thermometer (emissivity 0.95, TN408LC, OneTemp, Sydney Australia).

An ortho-rectified, 5 m pixel resolution, RapidEye satellite image (Jung-Rothenhaeusler et al. 2007) of the field was also acquired on the 3rd of February (2 days prior to the Raptor MkII survey). The NIR (760–850 nm) and Red (630–685 nm) bands were used to construct the SR image for comparison with the Raptor MkII image.

A point-to-point comparison of the Raptor MkII and RapidEye satellite data was conducted by overlaying the individual Raptor data points with the RapidEye pixels. Given the Raptor footprint size is comparable to the RapidEye pixel, a 5 m radius buffer was created around the geographic centre of every Raptor point (the instantaneous aircraft location), and the average SR of the RapidEye pixels determined within each buffer zone. This was done to allow for the possibility of mixed pixels lying with the instantaneous Raptor sensor footprint, as well as to accommodate the fact that the actual Raptor footprint on the ground may differ from the instantaneous aircraft location due to aircraft tilt/roll and GPS errors (Lamb et al. 2009). There was no additional irrigation between the satellite and Raptor sensor overflights.

Results and discussion

Optical sensor

The Raptor and RapidEye maps of the target field are given in Fig. 2.

Both maps have the same gross features in terms of zones of high and low SR values. Indeed even the irrigator wheel tracks (horizontal striping) is observable in the interpolated Raptor MkII map.

A scatterplot showing relationship between the coincident Raptor MKII and RapidEye SR data values is given in Fig. 3A, including a 1:1 line (dashed black line). Clearly the majority of the coincident RapidEye SR values are lower than the Raptor values. However, the RapidEye band values used to calculate the SR are top-of-atmosphere values and neglect any contribution of path radiance (atmospheric scattering; haze) to the incoming flux at the detector. Path radiance is expected to provide an additional offset to the pixel values, and more so at shorter wavelengths owing to Rayleigh scattering (Slater 1980). To this end one would expect the SR value, involving the ratio of a higher wavelength pixel value (NIR) to a lower wavelength (Red) value to be reduced compared to that with no path radiance effects. Numerous researchers have examined path radiance contributions to satellite imagery. A discussion of the numerous ‘in-scene’ techniques for correcting for path radiance in satellite imagery, namely those that do not involve/require measurement of the properties of the atmosphere (for example aerosol content) or the ground (e.g. surface reflectance), have recently been presented in Cheng et al. (2012). In many cases, the path radiance components in the NIR bands are largely ignored; assumed to be zero and a raster correlation plot between shorter-wavelength bands, for example the Red band, and an NIR band is a convenient means of estimating the path radiance component of the shorter-wavelength band from the Red band axis intercept. To this end, a raster correlation between the Red and NIR bands of the RapidEye scene used in this present work yielded a Red-axis intercept of 866 (digital number) which, when applied to the RapidEye pixel

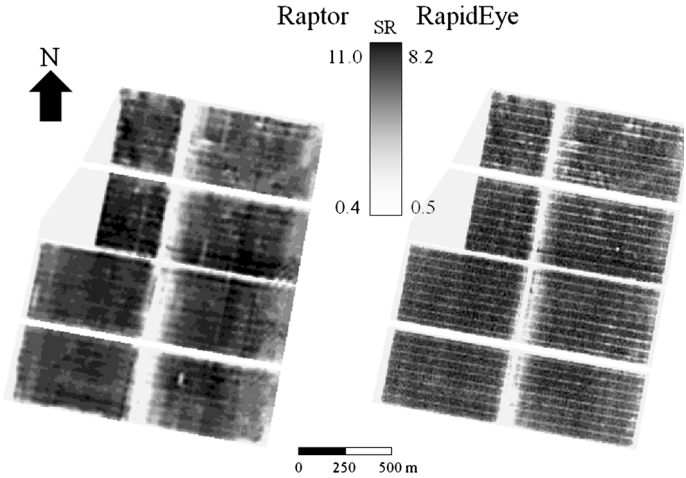

Fig. 2 A visual comparison between the derived SR map from the Raptor MkII sensor and the RapidEye satellite image. The colour ramp used to render the maps is based on an equal, 10-interval, grey-scale ramp applied between the indicated limits

values of the candidate field to recalculate the SR, yields the scatterplot in Fig. 3B which more closely follows the 1:1 line ($R^2 = 0.71$).

We believe the scatter around the 1:1 line is primarily the result of the different spatial resolution of the two sensors, specifically the fact that the smaller footprint of the Raptor sensor allows it to sense the inter-row soil. However there may also be a noise component introduced owing to the differences between the wavebands of the sensors. The LED-based Raptor sensor emits in relatively narrow wavelengths centered on 660 nm (Red) and 850 nm (NIR) [$\Delta\lambda \approx 18$ and 32 nm, respectively (Lamb et al. 2011)] compared to the comparatively broader RapidEye wavebands centred on 657 and 805 nm ($\Delta\lambda \approx 55$ and 90 nm, respectively). The red wavelength centres are virtually the same when considering the broad reflectance minima owing to chlorophyll absorption in the plant canopy. However it is possible the RapidEye Red waveband may include the region of rising reflectance between the red absorption minima and the chlorophyll red-edge of the plant's reflectance spectrum. There is a larger difference in the NIR central wavelengths but the NIR reflectance spectra of these plants (as is the case for most plants) is 'flat' out beyond 760 nm (up until 1 000 nm). However it is possible the RapidEye NIR band may be extending down in wavelength to the sloping region of the reflectance spectra between the 'red edge' and the NIR reflectance plateau.

Thermal sensor

The surface temperature map of the field derived from the Raptor MKII data is depicted in Fig. 4. The cotton crop canopy temperature varied between 24 and 30 °C, while the large areas of high temperature ($\sim$50 °C) are bare soil; such high surface temperatures of black vertosol soil are commonplace in this region (McKenzie 1998). These temperature ranges were subsequently verified by the spot measurements of canopy and bare soil surface temperature.

A visual comparison of Figs. 3A and 4 confirms the expected correlation between a lower canopy temperature and higher level of photosynthetically active biomass as

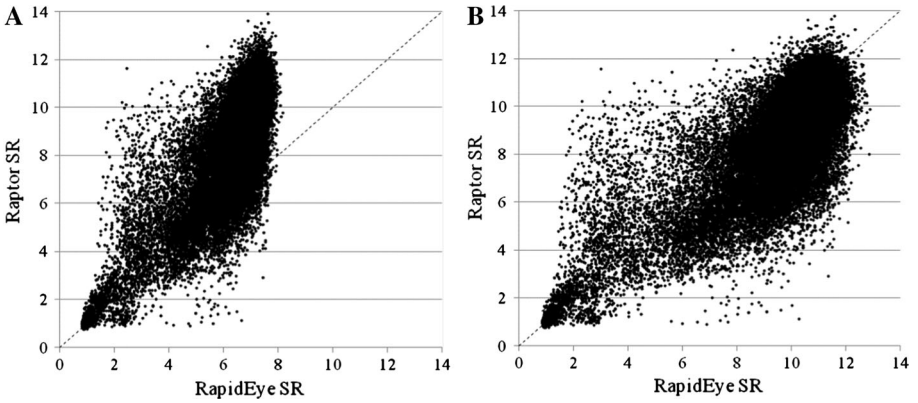

Fig. 3 Scatterplot of coincident Raptor SR values versus RapidEye satellite SR values (**A**) without and (**B**) with subtraction of estimated path radiance component from the RapidEye Red band ($R^2 = 0.71$). The 1:1 'agreement' line in each plot is depicted as a diagonal *dashed black line*

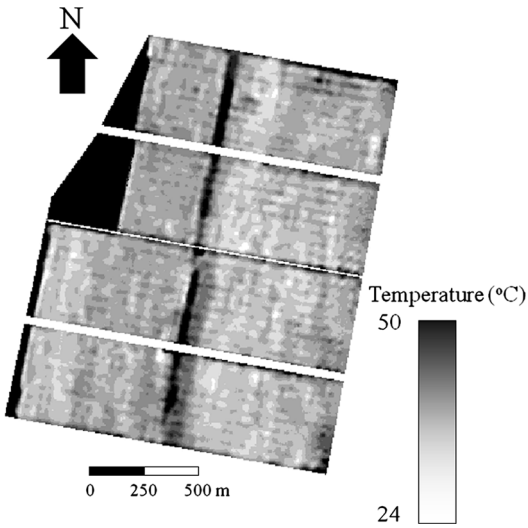

Fig. 4 Surface temperature map derived from the passive thermal sensor. The large areas of high temperature (*black*) are bare soil, of surface temperature ~50 °C. Plant canopy temperature varies between 24 and 30 °C

indicated by a higher value of SR. A scatterplot of the coincident SR and temperature values as recorded by the Raptor MkII sensor is given in Fig. 5. This plot conforms to the typical trapezoidal response curve observed in temperature-reflectance index correlation plots (Moran et al. 1994; Sandholt et al. 2002; Patel et al. 2009). A visual inspection of the field confirmed the scatter-plot presents the same zonal features as related to full to partial plant cover (Zone A) and partial plant cover to bare soil (Zone B) as outlined by Sandholt et al. (2002).

Conclusion

An integrated active optical (Red/NIR) and passive thermal sensor has been tested on a low-level aircraft for recording and mapping the reflectance and surface temperature

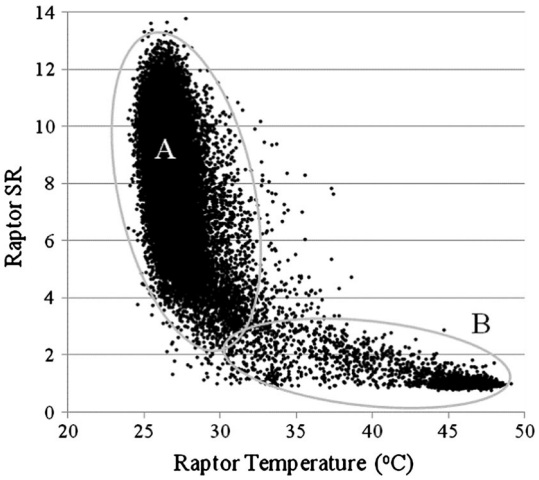

Fig. 5 Scatter plot of SR versus surface temperature for the coincident data points as collected by the Raptor MkII sensor over the entire field (~40 000 points). *Zones A* and *B* indicate regions of the field with full to partial plant cover and partial plant cover to bare soil, respectively

characteristics of a cotton crop from an altitude of 50 m above the canopy. An evaluation of the SR vegetation index map derived from the interpolated Raptor data against a RapidEye satellite image of the same field demonstrated not only equivalence between the two datasets, but also illustrated the shortfalls of the satellite image itself, namely the effects of path radiance. Indeed the Raptor MKII sensor is capable of providing scene-specific corrections to top-of-atmosphere satellite imagery and this will be the subject of further investigation. The passive thermal sensor on the Raptor MkII sensor provided canopy temperature values consistent with in situ, point field measurements.

An important advantage of this sensor over many satellite and airborne optical-thermal imaging systems is that the measurements of temperature are spatially coincident with the active optical reflectance measurements. As such, this integrated sensor is a potential alternative technology for determining plant and soil moisture status, at high spatial resolution, through the reflectance index-surface temperature approach that has been described previously by other workers using low spatial resolution systems (for example Sandholt et al. 2002).

From an operational perspective, this sensor can be retrofitted to any aerial top-dressing aircraft and data collection included in regular top-dressing operations.

Acknowledgments This work was funded by the CRC for Spatial Information (CRCSI), established and supported under the Australian Government Cooperative Research Centres Programme. The authors wish to acknowledge the technical support of Kyle Holland (Holland Scientific) in designing and building the Raptor™ Mk II sensor, David Boundy and Rob Maslen (Superair) for mounting the sensor on the aircraft and conducting the aerial surveys, Tim Neale (PrecisionAgriculture.com) for provision of the RapidEye satellite imagery and Nick Gillingham (Sundown Pastoral Company) for providing access to the field site. Specific mention of product brand names (e.g. CropCircle™ and Raptor™) or service providers (e.g. Holland Scientific or Superair) does not constitute an endorsement of these particular products or service providers. The authors declare that they have no conflict of interest.

References

Barker, D. W., & Sawyer, J. E. (2012). Using active canopy sensing to adjust nitrogen application rate in corn. *Agronomy Journal, 104*(4), 926–933.

Blum, A., Mayer, J., & Gozlan, G. (1982). Infrared thermal sensing of plant canopies as a screening technique for dehydration avoidance in wheat. *Field Crops Research, 5*, 137–146.

Cheng, K. S., Su, Y. F., Yeh, H. C., Chang, J. H., & Hung, W. C. (2012). A path radiance estimation algorithm using reflectance measurements in radiometric control areas. *International Journal of Remote Sensing, 33*(5), 1543–1566.

Falzon, G., Lamb, D. W., & Schneider, D. (2012). The Dynamic Aerial Survey algorithm architecture and its use in airborne fertilizer applications. *IEEE Journal of Selected Topics in Applied Earth Observations and Remote Sensing, 5*(6), 1772–1779.

Holland, K. H., Lamb, D. W., & Schepers, J. S. (2012). Radiometry of proximal active optical sensors (AOS) for agricultural sensing. *IEEE Journal of Selected Topics in Applied Earth Observations and Remote Sensing, 5*(6), 1793–1802.

Holland, K. H., & Schepers, J. S. (2010). Derivation of a variable rate nitrogen application model for in-season fertilization of corn. *Agronomy Journal, 102*, 1415–1424.

Holland, K. H. & Schepers, J. S. (2011). Active proximal sensing: Review of waveband selection, vegetation indices, scientific trump cards, etc., In "Proceedings of the ASA CSSA SSSA 2011 International Annual Meetings" (ASA, CSSA & SSSA: Madison, WI, USA), Paper 61–1.

Holland, K. H., & Schepers, J. S. (2013). Use of a virtual-reference concept to interpret active crop canopy sensor data. *Precision Agriculture, 14*(1), 71–85.

Holland, K. H., Schepers, J. S., Shanahan, J. F., & Horst, G. L. (2004). Plant canopy sensor with modulated polychromatic light source. In Mulla D. J. (Ed.), In Proceedings of the 7th International Conference on Precision Agriculture and Other Precision Resources Management, University of Minnesota, MN, USA: Department of Soil, Water and Climate.

Inman, D., Khosla, R., & Mayfield, T. (2005). On-the-go active remote sensing for efficient crop nitrogen management. *Sensor Review, 25*(3), 209–214.

Jackson, R. D., Idso, S. B., Beginato, R. J., & Pinter, P. J. (1981). Canopy temperature as a crop water stress indicator. *Water Resources Research, 17*, 1133–1138.

Jones, H. G. (2004). Irrigation scheduling: Advantages and pitfalls of plant based methods. *Journal of Experimental Botany, 55*(407), 2427–2436.

Jones, H. G., Archer, N., Rotenberg, E., & Casa, R. (2003). Radiation measurement for plant ecophysiology. *Journal of Experimental Botany, 54*(384), 879–889.

Jones, H. G., Serraj, R., Loveys, B. R., Xiong, L., Wheaton, A., & Price, A. H. (2009). Thermal infrared imaging of crop canopies for the remote diagnosis and quantification of plant responses to water stress in the field. *Functional Plant Biology, 36*, 978–989.

Jordan, C. F. (1969). Derivation of leaf-area index from quality of light on the forest floor. *Ecology, 50*, 633–666.

Jung-Rothenhaeusler, F., Weichelt, H. & Pach, M. (2007). RapidEye. A novel approach to space borne geo-information solutions. In: ISPRS Hanover Workshop 2007. High-Resolution earth imaging for geo-spatial information. Hannover. http://www.ipi.uni-hannover.de/fileadmin/institut/pdf/Jung-roth_weichelt_pach.pdf. Accessed 8 May 2013.

Künnemeyer, R., Schaare, P. N., & Hanna, M. M. (2001). A simple reflectometer for on-farm pasture assessment. *Computers and Electronics in Agriculture, 31*, 125–136.

Lamb, D. W., Schneider, D. A., Trotter, M. G., Schaefer, M. T., & Yule, I. J. (2011). Extended-altitude, aerial mapping of crop NDVI using an active optical sensor: A case study using a Raptor™ sensor over Wheat. *Computers and Electronics in Agriculture, 77*, 69–73.

Lamb, D. W., Trotter, M. G., & Schneider, D. A. (2009). Ultra low-level airborne (ULLA) sensing of crop canopy reflectance: A case study using a CropCircle™ sensor. *Computers and Electronics in Agriculture, 69*, 86–91.

McKenzie, D. C. (1998). Soil management guide-SOILpak for cotton growers. (3rd Ed), Munroe, A. and Roberts, E. (Eds.), New South Wales Agriculture, Sydney, NSW Australia, 352 pp.

Moran, M. S., Clarke, T. R., Inoue, Y., & Vidal, A. (1994). Estimating crop water deficit using the relation between surface-air temperature and spectral vegetation index. *Remote Sensing of Environment, 49*, 246–263.

Patel, N. R., Anapashsha, R., Kumar, S., Saha, S. K., & Dadhwal, V. K. (2009). Assessing potential of MODIS derived temperature/vegetation condition index (TVDI) to infer soil moisture status. *International Journal of Remote Sensing, 30*, 23–39.

Pinter, P. J., Zipoli, G., Reginato, R. J., Jackson, R. D., Idso, S. B., & Hohman, J. P. (1990). Canopy temperature as an indicator of differential water use and yield performance among wheat cultivars. *Agricultural Water Management, 18*, 35–48.

Sandholt, I., Rasmussen, K., & Andersen, J. (2002). A simple interpretation of the surface temperature/ vegetation index space for assessment of surface moisture status. *Remote Sensing of Environment, 79*, 213–224.

Slater, P. N. (1980). *Remote sensing—optics and optical systems*. Reading: Addison Wesley Publishing Co.

Solari, F., Shanahan, J., Ferguson, R., Schepers, J., & Gitelson, A. (2008). Active sensor reflectance measurements of corn nitrogen status and yield potential. *Agronomy Journal, 100*, 571–579.

Trotter, M. G., Lamb, D. W., Donald, G. E., & Schneider, D. A. (2010). Active optical sensors for quantifying and mapping pasture biomass: A case study using red and near infrared waveband combinations from a CropCircle™ in Tall Fescue (*Festuca arundinacea*) pastures. *Crop and Pasture Science, 61*, 389–398.

Wang, X., Yang, W., Wheaton, A., Cooley, N., & Moran, B. (2010). Efficient registration of optical and IR images for automatic plant water stress assessment. *Computers and Electronics in Agriculture, 74*, 230–237.

Whelan, B. M., McBratney, A. B. & Minasny, B. (2001). VESPER-spatial prediction software for precision agriculture. In Grenier, G. and Blackmore S. (Eds.), ECPA2001. In Proceedings of the 3rd European Conference on Precision Agriculture (pp 139-144), Montpellier France: Agro-Montpellier.